



A floating collagen matrix triggers ring formation and stemness characteristics in human colorectal cancer organoids

Daniel Gerhard Wimmers^{a,b}, Kerstin Huebner^{a,b}, Trevor Dale^c, Aristeidis Papargyriou^{d,e,f}, Maximilian Reichert^{d,e,f,g,h,i,j}, Arndt Hartmann^{b,k,l}, Regine Schneider-Stock^{a,b,k,l,*}

^a Experimental Tumorpathology, Universitätsklinikum Erlangen, Friedrich-Alexander-Universität Erlangen-Nürnberg (FAU), Germany

^b Institute of Pathology, Universitätsklinikum Erlangen, Friedrich-Alexander-Universität Erlangen-Nürnberg (FAU), Germany

^c Cardiff University, European Cancer Stem Cell Research Institute (ECSCRI), School of Bioscience, Cardiff, United Kingdom

^d Translational Pancreatic Cancer Research Center, Klinik und Poliklinik für Innere Medizin II, Klinikum rechts der Isar, Technical University of Munich, Munich, Germany

^e Technical University of Munich, Klinik und Poliklinik für Innere Medizin II, Klinikum rechts der Isar, Munich, Germany

^f Institute of Stem Cell Research, Helmholtz Center Munich, German Research Center for Environmental Health, Neuherberg, 85764, Germany

^g Center for Organoid Systems, Technical University of Munich, Garching, Germany

^h Munich Institute of Biomedical Engineering (MIBE), Technical University of Munich, Garching, Germany

ⁱ German Center for Translational Cancer Research (DKTK), Munich, Germany

^j Bavarian Cancer Research Center (BZKF), Munich, Germany

^k Comprehensive Cancer Center Erlangen-EMN (CCC ER-EMN), Erlangen, Germany

^l Bavarian Cancer Research Center (BZKF), Erlangen, Germany

ARTICLE INFO

Keywords:

Collagen I
Matrigel
Stemness
Ring structures
Invasiveness
TROP2

ABSTRACT

Intestinal organoids reflect the 3D structure and function of their original tissues. Organoid are typically cultured in Matrigel, an extracellular matrix (ECM) mimicking the basement membrane, which is suitable for epithelial cells but does not accurately mimic the tumour microenvironment of colorectal cancer (CRC). The ECM and particularly collagen type I is crucial for CRC progression and invasiveness. Given that efforts to examine CRC organoid invasion in a more physiologically relevant ECM have been limited, we used a floating collagen type I matrix (FC) to study organoid invasion in three patient-derived CRC organoid lines. In FC gel, organoids contract, align, and fuse into macroscopic ring structures, initiating minor branch formation and invasion fronts, phenomena unique for the collagen ECM and otherwise not observed in Matrigel-grown CRC organoids. In contrast to Matrigel, FC organoids showed basal extrusion with improper actin localization, but without change in the organoid polarity. Moreover, small clusters of vital invading cells were observed. Gene expression analysis revealed that the organoids cultured in a FC matrix presented more epithelial and stem cell-like characteristics. This novel technique of cultivating CRC organoids in a FC matrix represents an *in-vitro* model for studying cancer organization and matrix remodelling with increased organoid stemness potential.

1. Introduction

Intestinal organoids comprise the 3D architecture and organ-specific function of the originating organ. To date, the extracellular matrix (ECM) mainly used for the cultivation of intestinal organoids is Matrigel, a gelatinous protein mixture with poorly defined ingredients. As its main components are collagen type IV and laminin, it mimics the basement membrane, which makes it a suitable matrix for growing organoids from

epithelial cells. However, it does not accurately reflect the tumour microenvironment (TME) surrounding colorectal cancer (CRC) cells [1]. The growth and progression of colorectal tumours are strongly influenced by their surrounding ECM and particularly collagen I, plays a crucial role by influencing various processes such as metastasis [2], genomic instability [3], drug resistance [4], or immune infiltration [5] and thus contributing to malignant transformation [5]. During these processes, cancer cells not only take advantage of the collagen in the

* Corresponding author at: Experimental Tumorpathology, Universitätsklinikum Erlangen, Friedrich-Alexander-Universität Erlangen-Nürnberg (FAU), Germany.
E-mail address: regine.schneider-stock@uk-erlangen.de (R. Schneider-Stock).

<https://doi.org/10.1016/j.prp.2025.155890>

Received 11 October 2024; Received in revised form 6 February 2025; Accepted 1 March 2025

Available online 3 March 2025

0344-0338/© 2025 The Authors. Published by Elsevier GmbH. This is an open access article under the CC BY license (<http://creativecommons.org/licenses/by/4.0/>).

stroma but also promote collagen deposition by cancer-associated fibroblasts to increase matrix stiffness, another known ECM-driven mechanism to tumour aggressiveness [6].

In addition to its prominent role in CRC tumour progression, collagen I constitutes a more physiological alternative to Matrigel and contributes to increased reproducibility, as it eliminates batch-to-batch variability. As organoids become increasingly refined, new methods are needed to map the complex structure and behaviour of tumours [7]. However, to date, only limited efforts have been made to further develop existing organoid model systems.

Here, we present the cultivation of three patient-derived CRC organoids in a floating collagen type I (FC) matrix. It is a novel protocol for cultivation of human colorectal cancer organoids based on its original description in mouse small intestine organoids [8]. This simple method

enables cystic CRC organoids to form macroscopic ring structures with enhanced stemness characteristics. Moreover, physiological cancer cell phenomena such as matrix invasion and basal-cell extrusion can be observed.

2. Results and discussion

2.1. Organoids with cystic morphology form ring structures in a floating collagen matrix

In this study, we tested the behaviour of three patient-derived CRC organoid lines with different tumour stages and metastatic status when cultivated in a floating collagen (FC) type I matrix compared to Matrigel (Fig. 1A-B, Fig. S1). Organoids from healthy colorectal tissue as well as

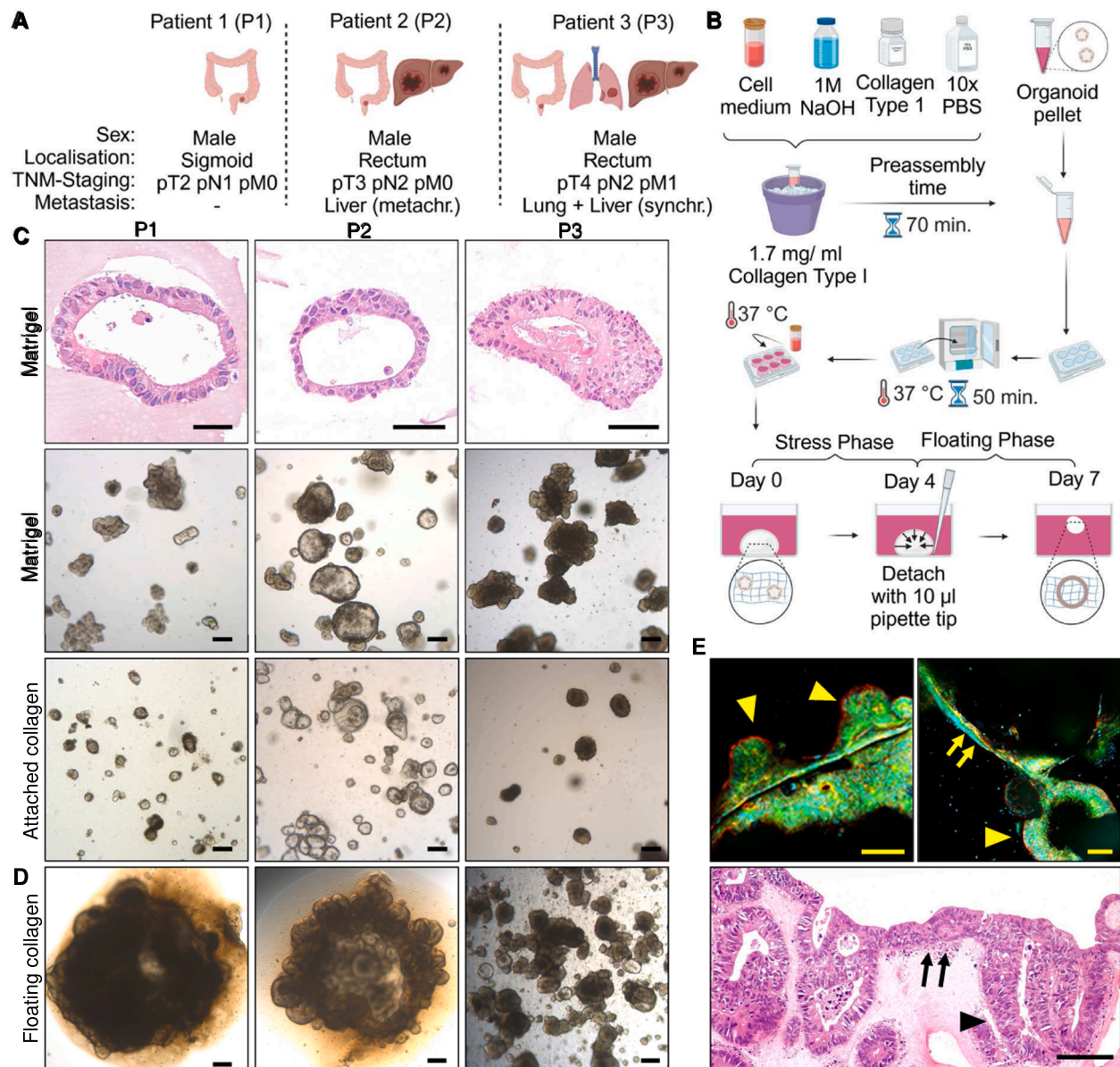


Fig. 1. Comparison of cultivation in Matrigel, attached collagen, and floating collagen. (A) Clinicopathological data of the three patient-derived organoid lines (P1–P3) used in this study; metachr.-metachronous; synchr.-synchronous. (B) Workflow for the generation of the floating collagen (FC) matrix. (C) Representative histological (HE, top panel) of organoid lines P1–P3 in Matrigel; brightfield images (middle and lower panel) of independent experiments of the organoid lines P1–P3 cultured in Matrigel and in attached collagen. Scale bars: 50 µm (top panel); 200 µm (middle and lower panels). (D) Representative brightfield images of the growth patterns of P1–P3 organoids in FC. Scale bars: 200 µm. (E) Representative immunofluorescence and histological (HE) images of P2 organoids (▲) in FC fused to the epithelium (†) of the ring structure. For whole-mount confocal imaging, the organoids were stained with phalloidin (red), tubulin (green), and DAPI (blue). Scale bars: 20 µm (top panel); 200 µm (lower panel).

CRC organoids grown in Matrigel typically grow as sharply defined cystic structures without visible interactions with neighbouring organoids or the surrounding matrix (Fig. 1C). A tumour-specific morphology is usually not visible. Collagen type I, as used in the associated collagen gel contraction assay (CGCA), is the preferred alternative matrix for CRC cultivation in a more physiological TME, especially for the transplantation of organoids into *in-vivo* mouse models [9]. Traditionally, researchers have used the attached-matrix model of CGCA with the collagen drop still being attached to the matrix so that the gel can only contract in the vertical dimension [10]. When cultivated in an attached collagen matrix, the overall morphology of the three organoid lines did not change, but some organoid clusters and fibre alignment around the organoids was visible (Fig. 1C). However, this interactive behaviour seemed to be restricted by the stiffness and inflexibility of the collagen matrix due to its attachment to the plate. In particular, the organoid line of patient one (P1) already showed some spontaneous detachment of the collagen drops.

For the first time, we cultivated CRC organoids in a modified version of the CGCA floating matrix model (Fig. 1B). During the first 4 days—the so-called “stress phase”—the organoids had the opportunity to grow and build tension in the collagen gel. To overcome the challenge of matrix inflexibility, the collagen drop was detached on day 4 to initiate the floating phase (Fig. 1B). This technique has been shown to enable murine small intestine organoids to interact not only with the matrix through contraction but also with each other to form tube- and crypt-like macroscopic superstructures [8]. In organoids derived from other tissues, including pancreatic cancer and breast, phenomena such as branching [11] or alveolation [12] can be observed. When our three patient-derived CRC organoid lines were cultivated in FC, the predominantly cystic organoid lines P1 and P2 fused to form macroscopic ring structures (Fig. 1D, E).

2.2. CRC organoid cultivation in FC allows long-term cultivation, matrix remodelling, and matrix invasion

Time lapse imaging over the course of 3 days postdetachment (p.d.) demonstrated the dynamics of ring formation in P1 organoids (Fig. 2A). During the first 16 h p.d., we observed significant collagen matrix contraction and organoid contact. A few organoids were already visible at the edge of the drop. Over time, the organoids further contracted the matrix, aligned, and an increasing number of organoids moved to the edge of the drop and merged into the developing ring structure. Due to the flat disc-like geometric structure of the FC matrix there is uniform nutrient access, eliminating nutrient gradient-driven organoid movement. The fusion to the epithelium of the ring was also visible via our immunofluorescence and histological analyses (Fig. 1E). The phenomenon of ring formation in the FC matrix was observed only in the P1 and P2 organoids, whereas the patient three (P3) organoids showed only minor contraction, consumption of the FC matrix and, rather, predominant organization into small groups. Various variables, such as stiffness, collagen concentration, and lack of cancer-associated fibroblasts [13] in FC compared to the primary tumour, could explain the differences in the behaviour of the three organoid lines. Strikingly, the ring structure in the FC drop could be maintained for up to 14 days, whereas the availability of free collagen matrix was the limiting factor due to collagen consumption and contraction by the organoids, as exemplified by P2 in Fig. 2B. Compared with attached collagen, the same organoid line survived for only 7 days until the organoids “burst” to eliminate debris and dead cells (Fig. 2B).

Strikingly, when two FC matrices contacted each other randomly (e.g. overnight at the edge of the well), the fusion of those two floating collagen drops was regularly observed (Fig. 2C). Microscopic analysis of the fused drops revealed that they were connected by a continuous

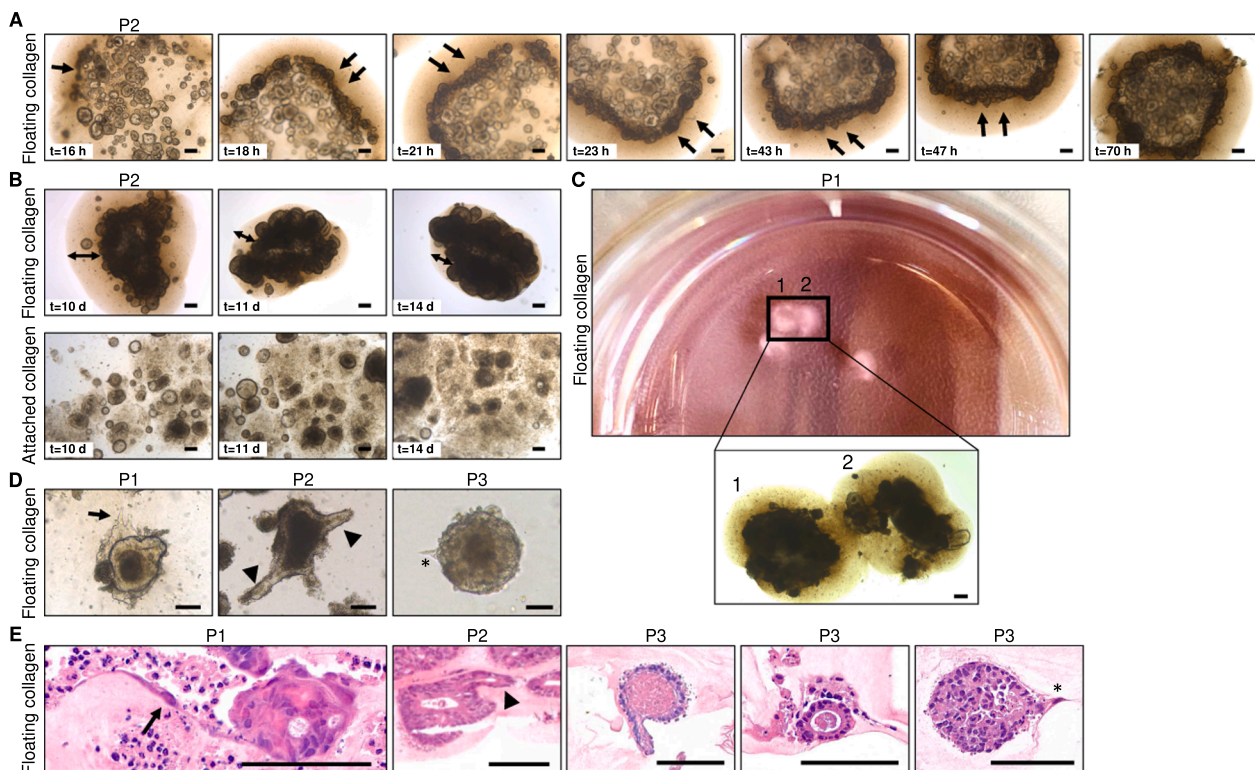


Fig. 2. Properties of the ring structures and matrix invasion. (A): Representative bright-field images of a P2 ring structure formed in floating collagen (FC) over the course of 70 h. Scale bars: 200 μ m. (B) Time-lapse bright-field imaging of P2 organoids over the course of four days in the final phase of cultivation in FC (top panel) and attached collagen (AC; no detachment step performed) (lower panel) at the same point of time in cultivation. Arrows (\leftrightarrow) highlight the contraction of the collagen matrix. Scale bars: 200 μ m. (C) Representative images of two fusing P1 FC organoid drops (1, 2). Scale bars: 200 μ m. (D) Brightfield images of various morphologically different invasion patterns into the collagen matrix in FC organoids (\uparrow , \blacktriangle , $*$). Scale bars: 200 μ m. (E) Histological findings of various FC matrix invasion patterns (\uparrow , \blacktriangle , $*$) observed by HE staining. Scale bars: 100 μ m.

bridge of fibres from the macroscopic organoid ring of one drop to the organoid ring of the other drop (Fig. 2C). These ring assemblies can be separated only by direct mechanical force from pipette tips. However, further research is necessary to understand the mechanism by which organoid structures in these two drops sense each other and remodel the matrix.

In addition to their morphological variety, some branching and invasion front-like structures that have never been observed in CRC organoids cultivated in Matrigel are also visible. The invasion of colorectal cancer cells into a collagen matrix, compared to Matrigel, was first reported by Vellinga et al. in an attached collagen matrix [14]. Friedl et al. described different morphological patterns of cancer invasion that were primarily shown in laboratory-intensive systems [15]. Friedl et al.

differ between individual and collective migration, where cell–cell adhesions are still retained [15]. Indeed, such a collective migration pattern of multicellular groups with small cell clusters or solid strand formation was visible in all 3 organoid lines via brightfield microscopy and immunohistochemical analysis (Fig. 2D, E). The organoid cells may have been chemoattracted by each other or simply followed microtracks in the FC matrix (Fig. 2D, E). Overall, the pattern of invasion was not patient specific. Since the protrusions exhibited highly temporal dynamics, with some of the fronts being visible for only hours, further imaging was complicated. We were not able to float Matrigel drops without damaging the matrix due to the low connectivity of proteins. In another study, a matrix similar to Matrigel floated, but FC-mediated invasion phenomena could not be observed [16].

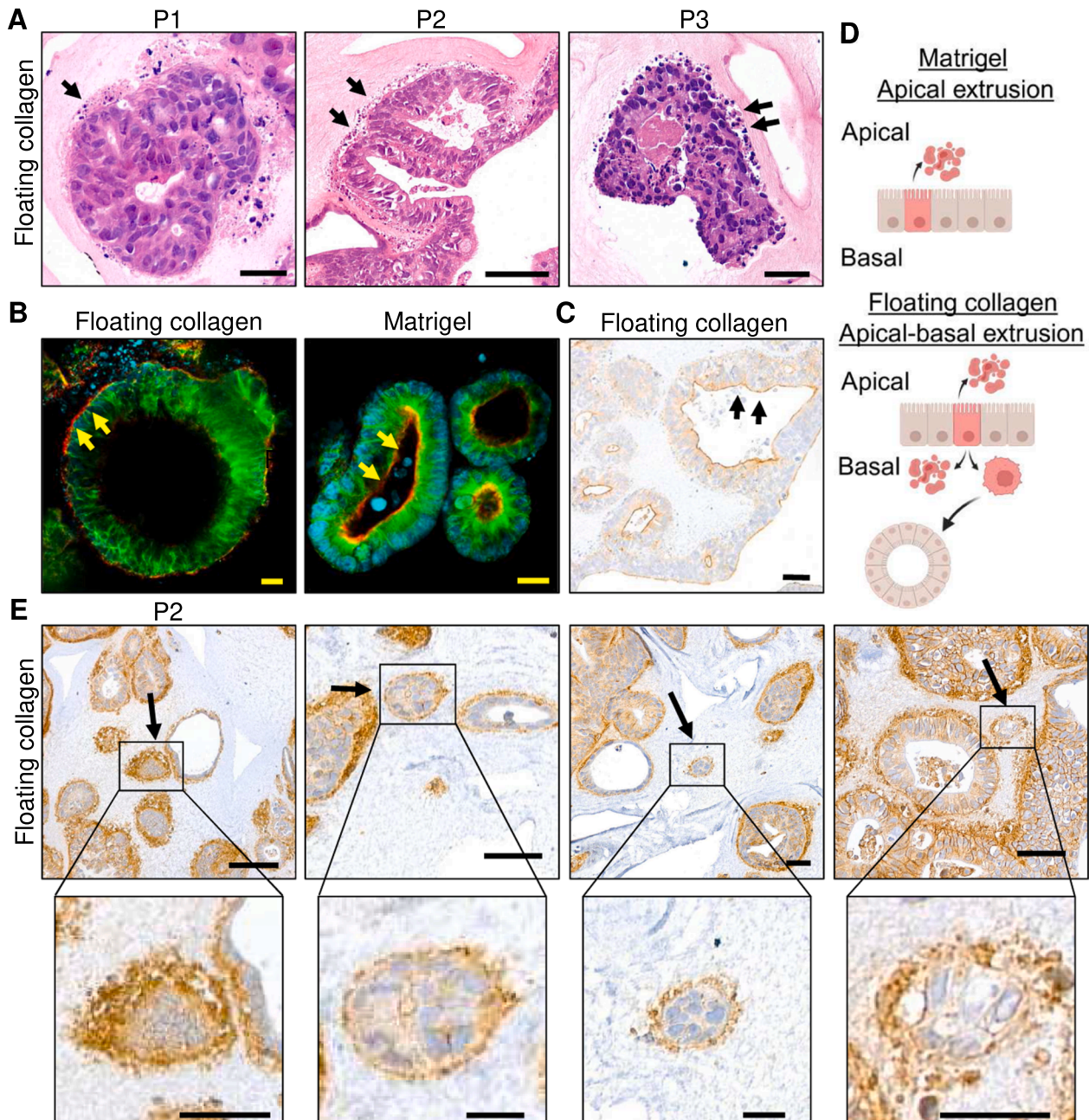


Fig. 3. Apical-basal extrusion in floating collagen organoids. (A) Cell debris surrounding P1–P3 organoids cultivated in FC as observed by HE staining (↑). Scale bars: 50 μ m. (B) Representative whole-mount confocal images of P2 organoids in Matrigel or in FC. Organoids were stained with phalloidin (red), tubulin (green), and DAPI (blue). Arrows (↑) highlight the localization of the actin ring. Scale bars: 20 μ m. (C) Villin immunohistochemical staining of P2 organoids in FC. Scale bar: 100 μ m. (D) Schematic overview of differences in the direction of extrusion between organoids cultivated in floating collagen (FC) and in Matrigel. (E) Different examples of small cluster of cells/ organoidsof EpCAM-stained P2 organoids in FC. Scale bars: 50 μ m (top panel); 25 μ m (lower panel).

2.3. Floating collagen organoids exhibit an apical-basal extrusion phenomenon

Epithelial cell extrusion is the process by which cells of the epithelium are removed to maintain a homeostatic epithelial cell number without disrupting the epithelial barrier. Typically, in healthy colonic tissue as well as in organoids cultured in Matrigel, cells are extruded apically by contraction of the apical actin ring of the neighbouring cell surrounding the apoptotic cell [17]. In CRC organoids grown in Matrigel, the apical side faces towards the lumen into which dead cells are shed (Fig. 1C); the same observation was reported in attached collagen drops [18]. Therefore, these organoids require frequent passaging to remove cell debris and maintain organoid viability. Unlike Matrigel-like organoids, FC organoids were surrounded by a flood of apoptotic bodies, as revealed in HE staining (Fig. 3A). To evaluate the role of F-actin in this phenomenon, we determined the localization of the actin filaments in P2 organoids by confocal immunofluorescence. We observed that the actin ring faced the apical side of the lumen in Matrigel, whereas in FC, the actin filament was instead localized on the basal side (Fig. 3B). Interestingly, the overall polarity of the organoid ring structures did not change upon cultivation in FC, as shown by Villin staining (Fig. 3C). Thus, for both conditions, the apical side of the organoids cultured in either Matrigel or FC still faced towards the lumen. Contrary mucinous colon cancer organoids cultivated in collagen I switched their apico-basal polarity [18].

So far, we can only speculate why both extrusion directions (Fig. 3D) occurred in FC (Fig. 3 A-C). In this context, an improper localization of the actin filaments was shown to randomize the direction of extrusion [17]. Moreover, a matrix containing collagen type 1 was an adequate

murine mammary organoid environment to study basal extrusion and breaching of the epithelium [19]. Fadul et al. (2018) reported that basal extrusion is a feature of highly invasive tumour cells and suggested a novel mechanism of metastasis [20]. Indeed, our histological analysis revealed the presence of small groups of tumour cells in the FC matrix after more than 9 days of cultivation (corresponds to 5 days p.d.) (Fig. 3E). This phenomenon has never been observed in Matrigel. We suggest that such cell clusters survive anoikis signals and are capable of forming new organoids, a phenomenon that has already been described by Vellinga et al. (2016). Single-cell approaches such as spatial scRNA-seq are necessary to further decipher the molecular profile and mechanism of these invading cancer cells.

2.4. Cultivation of organoids in an FC matrix triggers stemness characteristics

Organoids cultivated in Matrigel are frequently used as versatile model systems to recapitulate the gene expression signature and morphological and functional features of the corresponding cancer cells *in-vitro* [21]. However, only a high-collagen TME contributes to cancer progression and metastasis and therefore fully reflects the invasion processes occurring *in-vivo*. In particular, the microenvironment of normal tissue, which is reflected by the Matrigel composition, can reduce if not compensate for the effects of aggressive oncogenic drivers in epithelial cells [22].

As collagen has been shown to inhibit differentiation and trigger stemness in colorectal cancer cells [23], we aimed to better understand the observed morphological changes at the molecular level. Therefore, we defined 4 sets of genes for qPCR analysis, including stem cell,

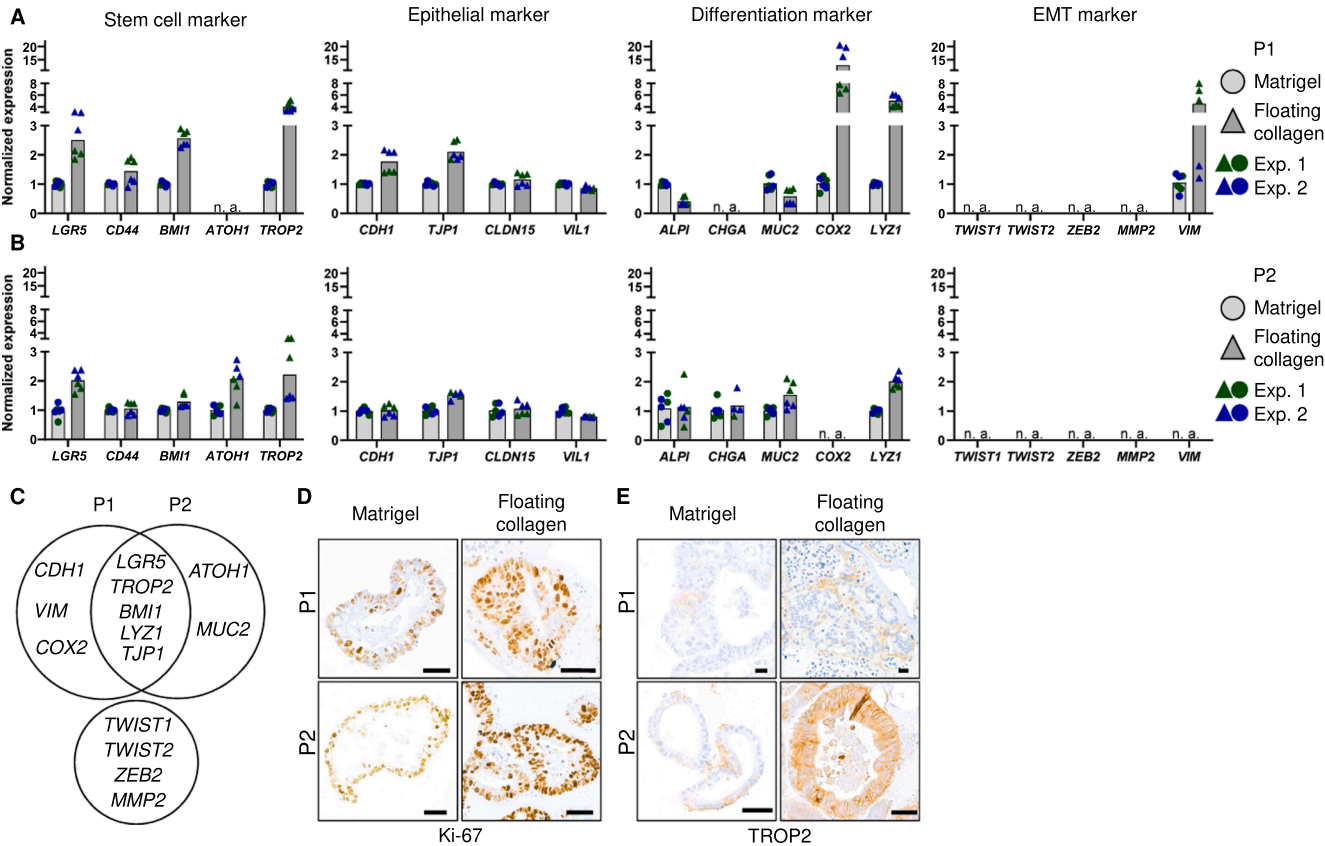


Fig. 4. Molecular characteristics of the organoid ring structures. (A-B) qPCR analysis of the gene sets for stemness, epithelial, differentiation, and EMT markers for P1 (A) and P2 (B) organoids cultivated in floating collagen (FC) and Matrigel. mRNA levels were normalized to GAPDH and calculated relative to those of the Matrigel condition on day 9 of cultivation. Data from two independent experiments (three technical replicates each, two colour codes; Exp.- experiment) are shown as single data points and the mean. (C) Venn diagram of upregulated genes for P1 and P2 organoids in FC. (D-E) Immunohistochemical comparison of Ki67 (D; proliferation marker) and TROP2 (E) expression in P1 and P2 organoids in Matrigel or FC.

epithelial, differentiation, and EMT markers (Fig. 4A, B). By analysing 9-day-old organoids (\pm 5 days p.d.), we observed an upregulation of the stem cell markers *LGR5*, *TROP2*, and *BMI1* in the FC organoids of P1 and P2 and *ATOH1* in P1 compared with Matrigel.

Although changes in gene expression upon cultivation in floating collagen were restricted to stemness, patient-specific gene expression alterations could be observed (Fig. 4C). While P2 organoids presented an increase in the expression of secretory markers such as *ATOH1* and *MUC2*, P1 organoids presented a rather inflammatory profile with an increase in *COX2* expression. In this context, *ATOH1*-positive secretory progenitor cells contribute to tissue homeostasis and renewal [24] whereas an increase in the most abundant *COX2* derivative *PGE2* promoted the organoid-forming efficiency and viability of *LGR5*⁺ intestinal stem cells [25]. Interestingly, P1 organoids presented increased *VIM* expression levels. These variable patterns in gene expression might reflect the different molecular subtypes of colorectal carcinomas [26].

Another important prognostic parameter is Ki-67 (a proliferation marker), which is associated with poor clinical outcomes in patients with CRC [27]. Our immunohistochemical staining results revealed strong Ki-67 expression in the Matrigel as well as in the FC P1 and P2 organoids, reflecting the strong proliferative activity of the two organoid lines under both conditions (Fig. 4D).

An interesting commonly upregulated marker in ring-forming lines is *TACSTD2*, which encodes the protein TROP2 and is a marker for foetal stem/progenitor cells [28] (Fig. 4C). In addition, we validated the increase in TROP2 expression at the protein level, as shown by TROP2 immunohistochemical staining (Fig. 4E). Its expression is correlated with the epithelial phenotype and is negatively associated with EMT [29], which was confirmed by our gene expression analysis (Fig. 4A-E). Recently, TROP2 overexpression in premalignant and malignant CRC lesions was shown to be a marker for developmental reprogramming in neoplastic cells [30]. We reported that increased expression of TROP2 in colon cancer cells triggered cell de-adhesion as a first step in metastasis [31].

To understand whether these alterations in gene expression were caused by matrix-induced temporal cell plasticity or by permanent changes, FC collagen organoids were transferred back to Matrigel, and gene expression was analysed after two passages in Matrigel. As a result, the organoids derived from P1 and P2 presented a decrease in stem cell marker expression with a shift to a more Matrigel-like differentiation pattern (Fig. S2). In P2, *TACSTD2* expression was even below the original Matrigel level.

Overall, our results suggest that the cultivation of CRC organoids in a floating collagen matrix amplifies the existing organoid-specific gene expression profiles, thereby enabling the organoids to fully exploit their malignant potential within an interactive matrix system.

3. Conclusion

Our method of embedding patient-derived CRC organoids in a FC matrix allows for organoid self-organization into ring structures through matrix remodelling and contraction. In this approach, physiological cancer cell phenomena such as matrix invasion become detectable, which has never been previously observed in Matrigel. Compared with their Matrigel organoid counterparts, the generated ring structures have enhanced stem cell-like characteristics. The remarkable self-organization of organoids achieved by cultivation in FC constitutes the extension of macroscopic tumour formation to patient-derived CRC organoids.

4. Materials and methods

4.1. Human samples and ethical guidelines

The organoids of Patient 1 and Patient 2 were kind gifts from Prof. Trevor Dale (Cardiff University, Wales) and were recently published as

ISO49 and ISO50 [32]. The tissue used for the generation of organoids from Patient 3 was collected at the Universitätsklinikum Erlangen (Germany). All procedures were performed in accordance with the Declaration of Helsinki and were covered by an ethics vote of the Universitätsklinikum of the Friedrich-Alexander-Universität Erlangen--Nürnberg (23–2023-Br).

4.1.1. Establishment and cultivation of organoids from human CRC tissue

The tumour samples from Patient 3 were cut into small fragments and washed with 10 mL of 3 + medium (Table S1) in a Petri dish. Next, the fragments were transferred into a 15 mL Falcon tube, and 3 mL of complete digestion medium containing RPMI 1640 (PAN Biotech™), FBS (final concentration 5 %), collagenase XI (Vetec™, final concentration 5 mg/mL), Y-27632 (Stemcell Technologies™, final concentration 10.5 μ M) and DNase I (Stemcell Technologies™, final concentration 10 μ M) was added and incubated at 37 °C for 2 h. After digestion, the suspension was passed through a 40 μ L strainer (Falcon™) and centrifuged at 300 \times g at 4 °C for 5 min. Then, the supernatant was removed, and the sample was washed with 5 mL of 3 + medium. After centrifugation (300 \times g, 4 °C, 5 min), the supernatant was removed, and the cells were resuspended in an appropriate amount of growth factor-reduced Matrigel (Corning). The suspension was then plated on a 48-well plate (25 μ L per well), and after solidification (10–15 min), complete culture medium (Table S1) was added. Organoids generated from Patient 3 were cultivated in complete culture medium (Table S1) independent of the ECM and passaged in Matrigel every 7 days. Organoids generated from Patient 1 and Patient 2 were recently described by Badder et al. (named ISO49 and ISO50, respectively) and were cultured in minimal medium [32].

4.1.2. Cultivation of organoids in Matrigel

The cultivation of organoids from Patient 1 and Patient 2 in Matrigel (Corning) was performed as previously described [32] (Table S1). After passaging, Y-27632 (Stemcell Technologies™) was added to the medium, which was then first changed after 3 days and then changed every other day without the addition of Y-27632. The organoids of Patient 3 were also cultivated in Matrigel (Corning) and received complete culture medium (Table S1) following the same scheme of changing the medium used for Patients 1 and 2. In general, organoids were passaged every 7 days. All organoid lines were regularly tested for mycoplasma contamination using endpoint PCR (primer sequence forward: 5' -TGC ACC ATC TGT CAC TCT GTT AAC CTC- 3'; reverse: 5' -GGA GCA AAC AGG ATT AGA TAC CCT- 3') with a mycoplasma PCR positive control DNA from the Leibniz-Institute DSMZ.

4.1.3. Preparation of the collagen matrix

Acid-digested rat tail collagen type I (Corning) was neutralized with 1 N NaOH to a pH of 7.2–7.4 via pH indicator strips. The gel was subsequently diluted with 10x PBS (Gibco™) and minimal medium (Table S1) to a final concentration of 1.7 mg/mL.

4.1.4. Cultivation of organoids in attached and floating collagen

For cultivation in the floating collagen matrix, the collagen mixture was incubated for 70 min after neutralization to allow for a preassembly time. For transfer from Matrigel to collagen I, 7-day-old Matrigel organoids were harvested, washed with 3 + medium (Table S1), and mechanically disrupted into large fragments by pipetting up and down 15–20 times. After centrifugation (300 \times g, 5 min, 4 °C), the supernatant was removed, the cell pellet from the preassembled collagen was resuspended, and 25 μ L of the organoid-collagen I mixture was plated into a 6-well plate. For solidification, the drops were incubated at 37 °C for 50 min before the addition of the corresponding culture medium supplemented with 10.5 μ M Y-27632 (Stemcell Technologies™). The medium was changed after 3 days and then every other day without the addition of Y-27632. For the floating, on day 4 of cultivation, the drops were detached from the plate by using a 10 μ L pipette tip.

4.1.5. Recovery after cultivation in floating collagen

Seven days post-passaging in Matrigel, the organoids were transferred into the neutralized collagen matrix, detached on day 4 and cultivated until day 9. The organoids were subsequently released from the collagen matrix with collagenase XI (Vetec™, final concentration 2 mg/mL) and washed three times with 3 + medium (Table S1). Next, the organoids were embedded and cultivated in Matrigel for 3 days until passaging, followed by 9 days until RNA extraction.

4.1.6. Immunohistochemistry (IHC)

For immunohistochemistry, floating collagen drops at different time points were collected with a spatula. Then, each drop was fixed for 20 min with 4 % PFA and washed three times with PBS (PAN Biotech™) for 5 min. Matrigel organoids were collected and released from the Matrigel by using Cell Recovery Solution (Corning) according to the manufacturer's instructions. After fixation with 4 % PFA for 30 min, the organoids were encased with the Eprelia™ Cytoblock™ Cell Block Preparation System according to the manufacturer's instructions. Organoids mounted in the Cytoblock were then paraffin-embedded, and 1 µm thin sections were prepared. The slides were subsequently deparaffinized and rehydrated according to standard protocols of the Institute of Pathology (Universitätsklinikum Erlangen). Slides were stained in an automated setting with haematoxylin and eosin (HE) following validated IHC protocols. IHC staining for Villin (1:100, ab130751, Abcam), TROP2 (1:2000, ab214488, Abcam), and Ki-67 (1:2000, #12202, Cell Signaling Technologies) was conducted manually overnight after heat-induced antigen retrieval and peroxidase blocking. Subsequently, the slides were incubated with biotinylated secondary antibodies, detected with a VECTASTAIN Elite ABC Kit (Vector Laboratories) and DAB substrate (Dako/Agilent), and counterstained with haematoxylin.

4.1.7. Brightfield and whole-mount immunofluorescence microscopy

Brightfield microscopy of the organoids was performed on a Leica DMi1 microscope. For immunofluorescence staining, the collagen drop was fixed after 7 days of cultivation as described above and transferred to an 8-well glass bottom µ-slide (Ibidi). Matrigel organoids were directly cultivated on 8-well µ-slides (Ibidi) and fixed with 4 % PFA for 30 min. For blocking and permeabilization, the samples were incubated overnight in buffer containing 0.1 % BSA, 0.2 % Triton X-100 and 0.05 % Tween 20 in PBS. Next, the samples were incubated with Alexa Fluor 488-conjugated anti-Tubulin (1:500, ab195883, Abcam) overnight. The next day, the samples were stained with Actistain 555 (1:40, PHDH1, Cytoskeleton Inc.) for 1.5 h at room temperature (RT) and with DAPI (1:1000, MBD0015, Sigma—Aldrich) for 15 min at RT. Finally, Fluoromount™ (Sigma—Aldrich) was added to each well and allowed to solidify at RT for 1 h. Confocal imaging was performed on the Cell-Voyager™ CQ1 Benchtop High-Content Analysis System (Yokogawa).

4.1.8. qPCR

For gene expression analysis, the organoids were cultivated in Matrigel or in a floating collagen matrix for 9 days. Organoids were released from their matrix by using Cell Recovery Solution (Corning) for Matrigel or collagenase XI (Vetec™, final concentration 2 mg/mL) for collagen. Isolation of total RNA, cDNA synthesis, and qPCR were performed as previously described [31]. Briefly, total RNA from cell pellets was extracted via the QIAzol Lysis Reagent (Qiagen) combined with the RNeasy Mini Kit (Qiagen) according to the manufacturer's protocol. The quality of the purified RNA was initially assessed via a Nanodrop1000 (Thermo Fisher). Reverse transcription was performed via the QuantiTect Reverse Transcription Kit (Qiagen, Hilden, Germany). cDNA amplification was conducted via primers for targets of interest (Metabion; Table S2) and the QuantiTect SYBR®Green PCR Kit (Qiagen) according to the manufacturer's protocol. Ct expression values were determined via the CFX96™ Real-Time System (Bio-Rad). The obtained Ct values were normalized to human GAPDH expression.

4.1.9. DNA isolation and next-generation sequencing

Patient 3 organoids were cultivated for 7 days and released from Matrigel using Cell Recovery Solution (Corning). The isolation was performed via the NucleoSpin Tissue Mini kit for DNA from cells and tissue (Macherey Nagel) according to the manufacturer's instructions. The quality of the purified DNA was initially assessed via a Nanodrop1000 (Thermo Fisher). Next-generation sequencing was performed via the TruSight Oncology 500 Assay (Illumina) on a NextSeq 550 (Illumina) according to the manufacturer's instructions for genomic profiling of the organoids.

4.1.10. Statistical analysis

Statistical analyses were performed with GraphPad Prism v. 10 (GraphPad, San Diego, CA, USA). Every experiment was performed at least twice with three technical replicates each.

Funding

R.S.S. was supported by Deutsche Forschungsgemeinschaft No. 468812580 and by Bayerisch-Tschechische Hochschulagentur (BTHA-AP-2022-15 and BTHA-JC-2019-1). M.R. is supported by the German Research Foundation (Deutsche Forschungsgemeinschaft, RE 3723/6-1). M.R. is supported by the Federal Ministry of Education and Research (BMBF) and the projects SATURN3 (01KD2206P), QuE-MRT (13N16450) and FAIRPACT (01KD2208B). M.R. is supported by the DKTK (German Consortium for Translational Cancer Research) Strategic Initiative Organoid Platform. M.R. receives funding from the Bavarian Cancer Research Center (BZKF) Translational Group "SARIFA T3triangle" and BZKF Lighthouse Project "Preclinical Model Systems". K.H. has won the CENIBRA LAC Young Scientist Imaging Assay Jumpstarter Contest to use the CQ1 imaging platform.

CRediT authorship contribution statement

Dale Trevor: Methodology. **Papargyriou Aristeidis:** Methodology. **Reichert Maximilian:** Methodology. **Wimmers Daniel Gerhard:** Writing – original draft, Visualization, Validation, Methodology, Investigation, Formal analysis, Data curation. **Huebner Kerstin:** Supervision, Methodology. **Hartmann Arndt:** Validation. **Schneider-Stock Regine:** Writing – review & editing, Writing – original draft, Supervision, Resources, Project administration, Funding acquisition, Conceptualization.

Declaration of Competing Interest

The authors declare that they have no known competing financial interests or personal relationships that could have appeared to influence the work reported in this paper.

Acknowledgements

The present work was performed in partial fulfilment of the requirements for obtaining the degree „Dr. med.“ at the Universitätsklinikum Erlangen, Friedrich-Alexander-Universität Erlangen-Nürnberg (FAU). We are grateful to the group of Prof. Robert Stoeckl (Molecular Pathology, Institute of Pathology, Universitätsklinikum Erlangen) for performing next-generation sequencing of the Patient 3 organoid line. We thank Christa Winkelmann for her excellent technical assistance.

Appendix A. Supporting information

Supplementary data associated with this article can be found in the online version at [doi:10.1016/j.prp.2025.155890](https://doi.org/10.1016/j.prp.2025.155890).

References

- [1] S. Xu, H. Xu, W. Wang, S. Li, H. Li, T. Li, W. Zhang, X. Yu, L. Liu, The role of collagen in cancer: from bench to bedside, *J. Transl. Med.* 17 (2019) 309, <https://doi.org/10.1186/s12967-019-2058-1>.
- [2] X. Wu, J. Cai, Z. Zuo, J. Li, Collagen facilitates the colorectal cancer stemness and metastasis through an integrin/PI3K/AKT/snail signaling pathway, *Biomed. Pharm.* 114 (2019) 108708, <https://doi.org/10.1016/j.biopha.2019.108708>.
- [3] S. Ishihara, H. Haga, Matrix stiffness contributes to cancer progression by regulating transcription factors, *Cancers* 14 (2022) 1049, <https://doi.org/10.3390/cancers14041049>.
- [4] M. Franchi, K.A. Karamanos, C. Cappadone, N. Calonghi, N. Greco, L. Franchi, M. Onisto, V. Masola, Substrate type and concentration differently affect colon cancer cells ultrastructural morphology, EMT markers, and matrix degrading enzymes, *Biomolecules* 12 (2022) 1786, <https://doi.org/10.3390/biom12121786>.
- [5] M. Fang, J. Yuan, C. Peng, Y. Li, Collagen as a double-edged sword in tumor progression, *Tumour Biol.* 35 (2014) 2871–2882, <https://doi.org/10.1007/s13277-013-1511-7>.
- [6] J. Huang, L. Zhang, D. Wan, L. Zhou, S. Zheng, S. Lin, Y. Qiao, Extracellular matrix and its therapeutic potential for cancer treatment, *Signal Transduct. Target Ther.* 6 (2021) 153, <https://doi.org/10.1038/s41392-021-00544-0>.
- [7] K.M. Sullivan, E. Ko, E.M. Kim, W.C. Ballance, J.D. Ito, M. Chalifoux, Y.J. Kim, R. Bashir, H. Kong, Extracellular microenvironmental control for organoid assembly, *Tissue Eng. Part B Rev.* 28 (2022) 1209–1222, <https://doi.org/10.1089/ten.TEB.2021.0186>.
- [8] N. Sachs, Y. Tsukamoto, P. Kujala, P.J. Peters, H. Clevers, Intestinal epithelial organoids fuse to form self-organizing tubes in floating collagen gels, *Development* 144 (2017) 1107–1112, <https://doi.org/10.1242/dev.143933>.
- [9] A. Fumagalli, J. Drost, S.J. Suijkerbuijk, R. van Boxtel, J. de Lig, G.J. Offerhaus, H. Begthel, E. Beerling, E.H. Tan, O.J. Sansom, et al., Genetic dissection of colorectal cancer progression by orthotopic transplantation of engineered cancer organoids, *E2357-e2364, Proc. Natl. Acad. Sci. USA* 114 (2017), <https://doi.org/10.1073/pnas.1701219114>.
- [10] Q. Zhang, P. Wang, X. Fang, F. Lin, J. Fang, C. Xiong, Collagen gel contraction assays: from modelling wound healing to quantifying cellular interactions with three-dimensional extracellular matrices, *Eur. J. Cell Biol.* 101 (2022) 151253, <https://doi.org/10.1016/j.ejcb.2022.151253>.
- [11] S. Randriamanantsoa, A. Papargyriou, H.C. Maurer, K. Peschke, M. Schuster, G. Zecchin, K. Steiger, R. Öllinger, D. Saur, C. Scheel, et al., Spatiotemporal dynamics of self-organized branching in pancreas-derived organoids, *Nat. Commun.* 13 (2022) 5219, <https://doi.org/10.1038/s41467-022-32806-y>.
- [12] J.R. Linnemann, H. Miura, L.K. Meixner, M. Irmeler, U.J. Kloos, B. Hirschi, H. S. Bartsch, S. Sass, J. Beckers, F.J. Theis, et al., Quantification of regenerative potential in primary human mammary epithelial cells, *Development* 142 (2015) 3239–3251, <https://doi.org/10.1242/dev.123554>.
- [13] H. Kobayashi, K.A. Gieniec, T.R.M. Lannagan, T. Wang, N. Asai, Y. Mizutani, T. Iida, R. Ando, E.M. Thomas, A. Sakai, et al., The origin and contribution of cancer-associated fibroblasts in colorectal carcinogenesis, *Gastroenterology* 162 (2022) 890–906, <https://doi.org/10.1053/j.gastro.2021.11.037>.
- [14] T.T. Vellinga, S. den Uil, I.H. Rinkes, D. Marvin, B. Ponsioen, A. Alvarez-Varela, S. Fatrai, C. Scheele, D.A. Zwijsenburg, H. Snippert, et al., Collagen-rich stroma in aggressive colon tumors induces mesenchymal gene expression and tumor cell invasion, *Oncogene* 35 (2016) 5263–5271, <https://doi.org/10.1038/ncr.2016.60>.
- [15] P. Friedl, S. Alexander, Cancer invasion and the microenvironment: plasticity and reciprocity, *Cell* 147 (2011) 992–1009, <https://doi.org/10.1016/j.cell.2011.11.016>.
- [16] J.Y. Co, J.A. Klein, S. Kang, K.A. Homan, Suspended hydrogel culture as a method to scale up intestinal organoids, *Sci. Rep.* 13 (2023) 10412, <https://doi.org/10.1038/s41598-023-35657-9>.
- [17] G.M. Slattum, J. Rosenblatt, Tumour cell invasion: an emerging role for basal epithelial cell extrusion, *Nat. Rev. Cancer* 14 (2014) 495–501, <https://doi.org/10.1038/nrc3767>.
- [18] C. Canet-Jourdan, D.L. Pagès, C. Nguyen-Vigouroux, J. Cartry, O. Zajac, C. Desterke, J.B. Lopez, E. Gutierrez-Mateyron, N. Signolle, J. Adam, et al., Patient-derived organoids identify an apico-basolateral polarity switch associated with survival in colorectal cancer, *J. Cell Sci.* 135 (2022) jcs259256, <https://doi.org/10.1242/jcs.259256>.
- [19] C. Villeneuve, E. Lagoutte, L. de Plater, S. Mathieu, J.B. Manneville, J.L. Maître, P. Chavrier, C. Rossé, aPKC α triggers basal extrusion of luminal mammary epithelial cells by tuning contractility and vinculin localization at cell junctions, *Proc. Natl. Acad. Sci.* 116 (2019) 24108–24114, <https://doi.org/10.1073/pnas.1906779116>.
- [20] J. Fadul, J. Rosenblatt, The forces and fates of extruding cells, *Curr. Opin. Cell Biol.* 54 (2018) 66–71, <https://doi.org/10.1016/j.cob.2018.04.007>.
- [21] R. Wang, Y. Mao, W. Wang, X. Zhou, W. Wang, S. Gao, J. Li, L. Wen, W. Fu, F. Tang, Systematic evaluation of colorectal cancer organoid system by single-cell RNA-Seq analysis, *Genome Biol.* 23 (2022) 106, <https://doi.org/10.1186/s13059-022-02673-3>.
- [22] F. Zanconato, M. Cordenonsi, S. Piccolo, YAP and TAZ: a signalling hub of the tumour microenvironment, *Nat. Rev. Cancer* 19 (2019) 454–464, <https://doi.org/10.1038/s41568-019-0168-y>.
- [23] S.C. Kirkland, Type I collagen inhibits differentiation and promotes a stem cell-like phenotype in human colorectal carcinoma cells, *Br. J. Cancer* 101 (2009) 320–326, <https://doi.org/10.1038/sj.bjc.6605143>.
- [24] D. Castillo-Azofeifa, E.N. Fazio, R. Nattiv, H.J. Good, T. Wald, M.A. Pest, F.J. de Sauvage, O.D. Klein, S. Asfaha, Atoh1(+) secretory progenitors possess renewal capacity independent of Lgr5(+) cells during colonic regeneration, *Embo J.* 38 (2019) e99984, <https://doi.org/10.15252/emboj.201899984>.
- [25] C. Lee, M. An, J.G. Joung, W.Y. Park, D.K. Chang, Y.H. Kim, S.N. Hong, TNF α Induces LGR5+ stem cell dysfunction in patients with crohn's disease, *Cell Mol. Gastroenterol. Hepatol.* 13 (2022) 789–808, <https://doi.org/10.1016/j.jcmgh.2021.10.010>.
- [26] J. Guinney, R. Dienstmann, X. Wang, A. de Reyniès, A. Schlicker, C. Sonesson, L. Marisa, P. Roepman, G. Nyamundanda, P. Angelino, et al., The consensus molecular subtypes of colorectal cancer, *Nat. Med.* 21 (2015) 1350–1356, <https://doi.org/10.1038/nm.3967>.
- [27] Z.W. Luo, M.G. Zhu, Z.Q. Zhang, F.J. Ye, W.H. Huang, X.Z. Luo, Increased expression of Ki-67 is a poor prognostic marker for colorectal cancer patients: a meta analysis, *BMC Cancer* 19 (2019) 123, <https://doi.org/10.1186/s12885-019-5324-y>.
- [28] S. Yui, L. Azzolin, M. Maimets, M.T. Pedersen, R.P. Fordham, S.L. Hansen, H. L. Larsen, J. Guiu, M.R.P. Alves, C.F. Rundsten, et al., YAP/TAZ-dependent reprogramming of colonic epithelium links ECM remodeling to tissue regeneration, *Cell Stem Cell* 22 (2018) 35–49, <https://doi.org/10.1016/j.stem.2017.11.001>.
- [29] Y. Wen, D. Ouyang, Q. Zou, Q. Chen, N. Luo, H. He, M. Anwar, W. Yi, A literature review of the promising future of TROP2: a potential drug therapy target, *Ann. Transl. Med.* 10 (2022) 1403, <https://doi.org/10.21037/atm-22-5976>.
- [30] P. Bala, J.P. Rennhack, D. Aitymbayev, C. Morris, S.M. Moyer, G.N. Duronio, P. Doan, Z. Li, X. Liang, J.L. Hornick, et al., Aberrant cell state plasticity mediated by developmental reprogramming precedes colorectal cancer initiation, *Sci. Adv.* 9 (2023) eadf0927, <https://doi.org/10.1126/sciadv.adf0927>.
- [31] Huebner, Kerstin Erlenbach-Wuenssch, Katharina Prochazka, Ilir Jan, Sheraj, Chuanpit Hampel, Blanka Mrazkova, Tereza Michalcikova, Jolana Tureckova, Veronika Iatsiuk, Anne Weissmann, et al., ATF2 loss promotes tumor invasion in colorectal cancer cells via upregulation of cancer driver TROP2, *Cell. Mol. Life Sci.* 79 (2022) 423, <https://doi.org/10.1007/s00018-022-04445-5>.
- [32] L.M. Badder, A.J. Hollins, B. Herpers, K. Yan, K.B. Ewan, M. Thomas, J.R. Shone, D. A. Badder, M. Naven, K.E. Ashelford, et al., 3D imaging of colorectal cancer organoids identifies responses to tankyrase inhibitors, *PLoS One* 15 (2020) e0235319, <https://doi.org/10.1371/journal.pone.0235319>.